RESEARCH ARTICLE

The seasonal and spatial distribution of hydrochemical characteristics of groundwater and its controlling factors in the eastern Loess Plateau

Congjian Sun[1,2,3] · Wei Chen[1] · Yanjun Shen[3]

Abstract

Groundwater plays a key role in supplying water for drinking water, irrigation water, and industry water in the northern China. Recently, the availability and quality of groundwater resources in the eastern Loess Plateau (Shanxi province) have a serious impact on the agriculture, industry, and domestic sectors. This paper investigates the spatiotemporal variations of chemical and stable isotope composition of groundwater, and provides important information for the research of controlling factors of groundwater hydrochemical distribution in Shanxi province during two seasons. About 95 groundwater samples were collected from two seasons and measured the content of major ions and stable isotope, pH values, and total dissolved solids (TDS). The results showed that groundwater samples were mildly alkaline. Among all the groundwater samples, the HCO_3^- and Na^+ dominated the total mass of the anions and cations, respectively. Significant seasonal and spatial variations can be observed in the TDS, deuterium ($\delta^2 H$), and oxygen ($\delta^{18}O$) in groundwater samples. More pronounced variations of the groundwater TDS appeared in the quick-flow season with the highest TDS concentration observed at the central region and lower TDS values appeared in the northern and southern Shanxi. The groundwater samples mainly belong to the (HCO_3^--Ca^{2+}-Na^+) type and the (HCO_3^--SO_4^{2-}-Ca^{2+}-Na^+) type. Rock weathering is the key controlling factor for the chemical composition of groundwater. In addition, nitrogen pollution of groundwater caused by human input is more significant in river valley basins such as the Yuncheng Basin, Linfen Basin, and Changzhi Basin. The significant influence of surface water-groundwater interaction for the groundwater can be observed at the valley basin in the central part of the Shanxi Province. The interaction between surface water and groundwater in the Linfen basin is especially remarkable.

Keywords Groundwater · Hydrochemistry · Controlling factors · Surface water-groundwater interaction

✉ Congjian Sun
 suncongjian@sina.com

1 Shanxi Normal University, School of Geographical Science, No 1 Gongyuan Street, Linfen 041000, Shanxi, China

2 State Key Laboratory of Desert and Oasis Ecology, Xinjiang Institute of Ecology and Geography, Chinese Academy of Sciences (CAS), Urumqi 830011, Xinjiang, China

3 Key Laboratory of Agricultural Water Resources, Hebei Key Laboratory of Agricultural Water-Saving, Center for Agricultural Resources Research, Institute of Genetics and Developmental Biology, Chinese Academy of Sciences, 286, Huaizhong Road, Shijiazhuang 050021, China

Introduction

With the global warming intensification and rapid population growth, the shortage of water resources has become a common problem for most countries around the world (Li et al. 2011). China is one of the countries with the most serious water crisis in the world, especially in its arid and semi-arid area. The increasing water demand for agricultural irrigation and residents' living water lead to the continuous decline of groundwater level and the deterioration of groundwater environment in the northern China, which greatly promoted the research of groundwater hydrochemical (Li et al. 2011; Dogramaci et al. 2012; Xing et al. 2013). Understanding the spatial and temporal distribution of the hydrochemical and environmental isotope of groundwater is helpful for groundwater resource optimal allocation in one region (Li et al. 2011; Sun et al. 2016a, b, c). In most situations, monitoring the environmental isotopes and hydrochemical

characteristics of groundwater can provide valuable evidence and data for hydrological processes, especially by studying water routes, connectivity, transit time of water, transport of water and pollutants (Kattan. 2015, 2018; Sun et al. 2016a, 2017 and 2018). Geological conditions, quality of recharge water and input from other sources, chemical weathering degree of various rock types are considered to be important factors affection the chemical distribution and evolution of groundwater chemistry. The interaction among these controlled factors of groundwater chemical results in complex groundwater environment. The dissolution of minerals (including carbonates and silicates) and the precipitation of secondary minerals usually prevail in the basin scale (Sung et al. 2012; Xing et al. 2013). In the coastal plain, the hydrochemistry of groundwater will be affected by the seawater. Seawater with high salinity often flows backward into shallow groundwater because of the transitional extraction and utilization of shallow groundwater in coastal plain (Han et al. 2011; Liu et al. 2016; Sun et al. 2016a, b, c). At present, more and more research methods have been applied to the study of groundwater hydrochemical processes and geochemical evolution in the complex system such as: multivariate statistical analysis, Gibbs graph method, Piper third-line diagrams, water–rock interaction simulation and isotope hydrological separation. Using these methods, a lot of valuable information of groundwater environment around the world has been obtained (Beaucaire et al. 1995; Kumar et al. 2013; Stober 2014; Kattan 2015; 2018).

As the main supply center of energy source in China, Shanxi province has seriously affected its economic development and ecological security by the shortage of water resources. Since 1990s, groundwater has gradually become the main source of fresh water for agricultural, industrial and households needs because of the scarcity of precipitation, dry-up of rivers and the pollution of surface water (Tang et al. 2013). A large number of wells were built to pump groundwater from aquifers to cope with the enormous pressure of fresh water in recent years. Additional, groundwater level in some region which groundwater is excessive exploitation has fallen at alarming rates and appeared numerous drawdown cones (Xing et al. 2013). And then, the natural environment of groundwater system (including surface water-groundwater interaction, runoff and discharge conditions, hydrochemical characteristics and geochemical process) has obviously influenced by the decline of groundwater levels (Wang et al. 2018). The groundwater environment variation have threatened the sustainable usage of groundwater resources. Recently, groundwater environment variation in the northern China has attracted a lot of researchers' attention (Sung et al. 2012; Xing et al. 2013; Sun et al. 2016a, b&2017&2018). As for the Shanxi province, some researches of groundwater hydrochemical process has been carried out, but these studies mostly focus on the spatial and temporal distribution of groundwater hydrochemical and isotopic characteristics on the basin scale. There are few studies try to analysis the controlling abundant elements of the geochemical process, such as Fluoride (Hu et al. 2013) and Arsenic. In the eastern Loess Plateau, the geochemistry of iodine-rich groundwater of the southwest of the Taiyuan basin has been identified (Tang et al. 2013). As for the Linfen basin, the groundwater vulnerability in shallow aquifers has been assessed by using DRASTIC Model (Samake et al. 2011). However, Few hydrochemical and isotopic investigations in the whole eastern Loess Plateau (Shanxi province) (Wang et al. 2010).

In this study, we use the isotopic and hydrochemical tracers to assess groundwater chemical characteristic of different regions during a whole year. The specific objectives of the study were: (1) to analysis the spatial and seasonal variations of hydrochemical and isotopic characteristics of groundwater, (2) to determine the main mechanism controlling the groundwater geochemistry characteristics, and (3) to explore the effect of human activities on groundwater in Shanxi province. The results will help develop more suitable utilization strategies for groundwater resources in the northern China.

Material and methods

Study area

Shanxi Province locates the east of the Yellow River valley (between 34°36'- 40°44' N and 110°15' -114°32' E, the average altitude is 1, 450 m) and covers an area of 156,000 km^2 (Fig. 1). It has about 34 million people distribute in 119 counties. The annual air temperature ranges from -1 to 20 °C and the annual average precipitation amount is around 400–650 mm. Shanxi Province has an intricate topography and made up of higher ground to the west (lvliang Mountains) and the east (Taihang Mountains). The northern border is adjacent to Inner Mongolia and the Yellow River forms the western border of Shanxi with Shaanxi Province. In the center of the Shanxi Province, there are a series of valleys through with the Fen River runs, which include the Taiyuan Basin, Linfen Basin, Changzhi Basin, and Yuncheng Basin (Fig. 1). Drought environment and unreasonable utilization of water resources make the Shanxi province has severe security problems of water resources.

In order to better present the spatial and temporal distribution characteristics of groundwater hydrochemistry in Shanxi Province, we divided the study area into 6 regions, included the Northern Plateau, the Taiyuan Basin, the Linfen Basin, the Yuncheng Basin, the Lvliang Mountains, and the Changzhi Basin.

Fig. 1 Location of the study area and distribution of the sampling points in Shanxi Province of the eastern Loess Plateau
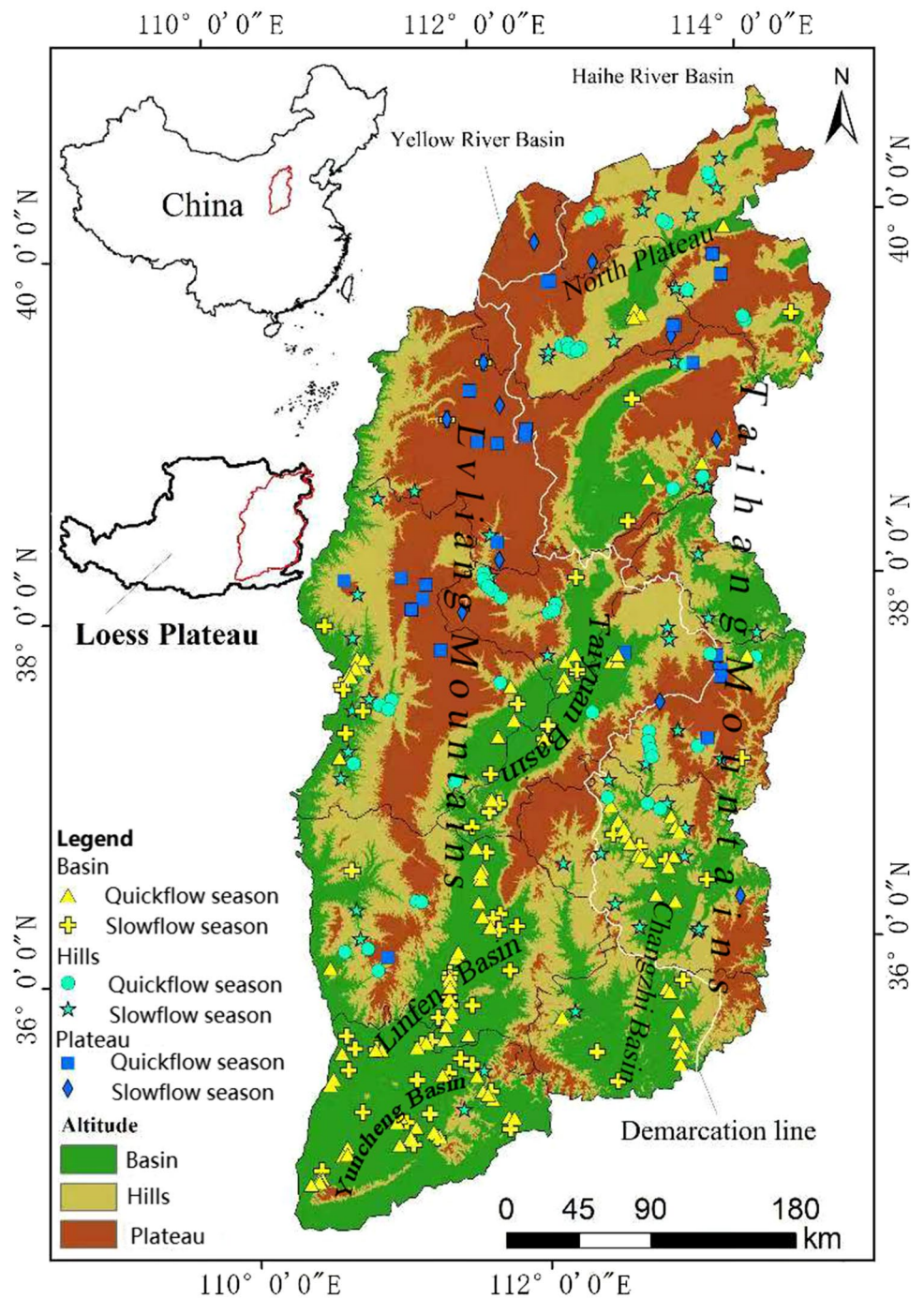
Sampling collection and analytical methods

The eastern Chinese Loess Plateau belongs to typical monsoon climate region, and regional hydrological processes presented significant seasonal variation between winter and summer. In order to reveal the spatiotemporal variation characteristics of groundwater environment in the study area, investigations were carried out between February 2017 (represented winter and slowflow season) and August 2017 (represented summer and quickflow season) and groundwater

samples were collected from 11 cities in Shanxi Province. A total of 95 samples were collected. 42 groundwater samples were collected in August 2017 and 53 groundwater samples were collected in February 2017. To clarification of complicated surface water-groundwater interactions, we collected 9 river water samples (3 samples were collected in February 2017 and 6 samples were collected in August 2017) and 9 precipitation samples (6 samples were collected in February 2017 and 3 samples were collected in August 2017) from Taiyuan basin, Linfen basin and Yuncheng basin during

two sampling periods (Table 1). Isotope water samples are preserved in 5-mL glass vials and sealed immediately with Parafilm to reduce evaporation. Each groundwater sample is collected at least 500 mL in plastic bottles for measuring major ion concentration of groundwater. The $\delta^{18}O$ and δD values and major ions values in the groundwater samples were measured at the State Key Laboratory of Desert and Oasis Ecology, Xinjiang Institute of Ecology and Geography, Chinese Academy of Sciences. The Liquid water Isotope Water Isotope Analyzer (Model DLT-100; Los Gatos Research lnc.) was used to measure $\delta^{18}O$ and δD values were analyzed by a Liquid Water Isotope Analyzer. The precision levels for $\delta^{18}O$ and δD were 0.1‰ and 0.3‰ respectively. Results were reported by the Vienna Standard Mean Ocean Water (V-SMOW). The major ion concentration of groundwater was determined by the dual-column instrument (Dionex DX-100), and the analytical errors were: Ca^{2+} (± 0.4 mg/L), Mg^{2+} (± 0.7 mg/L), Na^+ (± 0.1 mg/L), K^+ (± 0.1 mg/L), Cl^- (± 0.1 mg/L), SO_4^{2-} (± 0.3 mg/L), HCO_3^- (± 0.3 mg/L), and NO_3^- (± 0.1 mg/L).The analytical error was less than 1 mg/L. The water temperature, pH, and the total dissolved solids (TDS) values of all samples were measured in the field at the time of sampling.

In this study, the spatial and temporal variations of pH, TDS, major ion, and stable isotope are understood by the interpolation analysis in ArcGIS. Kriging interpolation method is used to map the spatial distribution of major ions in regional groundwater. Interpolation analysis can help us to make a more accurate analysis of component changes in groundwater in different seasons. Hydrochemical types were identified by the piper diagram. This method is composed of the percentages of the three main groups of main cations (Ca^{2+}, Mg^{2+}, $Na^+ + K^+$) and anions (Cl^-, SO_4^{2-}, $HCO_3^- + CO_3^-$) (Karmegam et al. 2011). The Gibbs graph defines the $Na^+/(Na^+ + Ca^{2+})$ or $Cl^-/(Cl^- + HCO_3^-)$ as the horizontal coordinate, and the TDS is the ordinate. The hydrochemical control factors are judged by the position of the scattered points (Gibbs, 1970).

EMMA (End Member Mixing Analysis) method is a widely used techniques which have been applied in research to identify the relationship between different water bodies. Owing to the results of EMMA, the three-component method was used to calculate the ratios of interaction between groundwater and various recharging water sources. The method can be described by following equations:

$$Q = \sum_{m=1}^{n} Qm$$
$$QC_b^b = \sum_{m=1}^{n} Q_m C_m^b \quad b = l, \ldots, k$$

where Q is total groundwater discharge, Q_m is the discharge of component m, and C_m^b is the tracer b incorporated into the component m.

Table 1 Statistical eigenvalues of hydrochemical parameters in Shanxi Province

Water type		Slowflow season					Quickflow season				
		Max	Min	Ave	SD	Cv	Max	Min	Ave	SD	Cv
Groundwater	pH	8.66	7.6	8.26	0.21	0.03	8.57	7.43	7.89	0.3	0.04
	$\delta^2H/‰$	-57.02	-86.26	-69.57	5.66	0.08	-58.35	-86.23	-72	5.31	0.07
	$\delta^{18}O/‰$	-9.2	-11.52	-8.98	0.7	0.3	-8.39	-11.48	-9.59	0.63	0.07
	TDS/ mg·L^{-1}	3040	149.7	915.15	512.8	0.56	2400	40.4	1013.78	508.71	0.5
	Na^+/ mg·L^{-1}	580.32	2.85	114.93	119.29	1.04	428.88	2.84	123.82	111.44	0.9
	K^+/ mg·L^{-1}	50.29	0.42	3.84	7.14	1.86	188	0.42	6.42	28.73	4.47
	Mg^{2+}/mg·L^{-1}	335.38	1.02	47.62	50.25	1.06	185.65	0.89	47.65	28.12	0.59
	Ca^{2+}/mg·L^{-1}	456.27	15.47	83.92	65.59	0.78	230.97	5.41	77.32	38.23	0.49
	Cl^-/mg·L^{-1}	458.39	1.78	79.19	91.42	1.15	450.84	0.02	111	109.87	0.99
	HCO_3^-/mg·L^{-1}	848.4	81.01	355.09	129.72	0.37	625.55	21.02	345.23	109.13	0.32
	SO_4^{2-}/mg·L^{-1}	802.12	6.69	176.22	169.8	0.96	708.26	3.89	161.78	124.86	0.77
	NO_3^-/mg·L^{-1}	169.69	1.32	49.93	47.16	0.94	321.64	0.31	123.95	87.81	0.71
River water	$\delta^2H/‰$	-63.55	-79.85	-70.71	6.78	0.10	-53.44	-62.13	-57.87	4.35	0.08
	$\delta^{18}O/‰$	-8.52	-11.17	-9.73	1.04	0.11	-7.71	-8.07	-7.84	0.20	0.03
	TDS/ mg·L^{-1}	1280.00	700.00	1030.00	218.94	0.21	1300.00	920.00	1154.33	204.93	0.18
Precipitation	$\delta^2H/‰$	-53.16	-62.49	-58.88	5.01	0.09	4.57	-45.46	-15.52	22.16	1.43
	$\delta^{18}O/‰$	-7.34	-8.58	-8.01	0.63	0.08	-0.13	-5.69	-2.34	3.10	1.32
	TDS/ mg·L^{-1}	90.00	74.00	80.83	8.25	0.10	121.00	93.00	105.33	15.82	0.15

Results

General hydrochemical characteristics of the study area

pH and TDS

In this study, the ranges of pH value in groundwater samples were 7.60–8.66 in slowflow season and 7.43–8.57 in quickflow season, which indicates the alkaline nature in Shanxi Province. The pH value during the quickflow season (with a mean of 7.89) is relatively lower than that of the slowflow season (with a mean of 8.26). The TDS recorded in the slowflow season and quickflow season ranged from 40.40 to 3,040 mg.L^{-1} with a coefficient of variation of 56% (Table 1), reflecting complex geographical environment of the study area. The relatively higher mean groundwater TDS value (1013.78 mg.L^{-1}) was observed in the quickflow season (915.15 mg.L^{-1}).

Major ion concentrations

The average, maximum, and minimum values of the content of inorganic ions in all groundwater samples are presented in Table 1. During the slowflow season, the main ion content of groundwater samples was in the following descending order: $HCO_3^- > SO_4^{2-} > Na^+ > Ca^{2+} > Cl^- > Mg^{2+} > K^+$ (contents are 355.09, 208.29, 114.93, 83.92, 79.19, 47.62, 3.84 mg·L^{-1}). In the quickflow season, the main ion content of groundwater samples was in the following descending order: $HCO_3^- > SO_4^{2-} > Na^+ > Cl^- > Ca^{2+} > Mg^{2+} > K^+$

(contents are 345.23, 161.78, 123.82, 111.00, 77.32, 47.65, 6.42 mg·L^{-1}). Among all the groundwater samples, the HCO_3^- and Na^+ dominated the total mass of the anions and cations, respectively. HCO_3^- occupies 55.3% of the total anion gross weight and Na^+ occupies 87% of the total cation gross weight. During the slowflow season, Na^+ dominated the total mass of the cations, occupying 46% of the total cations gross weight. Ca^{2+} was the second most substantial cation, occupying 33.5% of the aggregated total cations. HCO_3^- and SO_4^{2-} are the main anions of the groundwater samples for the slowflow season, occupying 53% and 26.7% of the total anion mass. During the quickflow season, Na^+ occupied 48.5% of the total cation gross weight. Ca^{2+} was the second most substantial cation, occupying 30.3% of the aggregated total cations. HCO_3^- and SO_4^{2-} are the main anions, occupying 46.5% and 21.8% of the total anion mass.

Seasonal and spatial variations of groundwater hydrochemistry

Figure 2 shows the spatial variations of pH and TDS during the two sampling periods. There is a clear difference in the pH spatial distribution patterns during the two sampling seasons. In the slowflow season, higher pH values appeared in the Lvliang Mountains and the lower pH values were observed in the eastern Shanxi Province. Obviously decrease trend for the pH values can be observed from west to east in the study area. During the quickflow season, the highest pH values with a range from 7.43 to 8.10 were observed in the northwestern Shanxi. The spatial variation pattern of groundwater TDS concentration is completely. In the
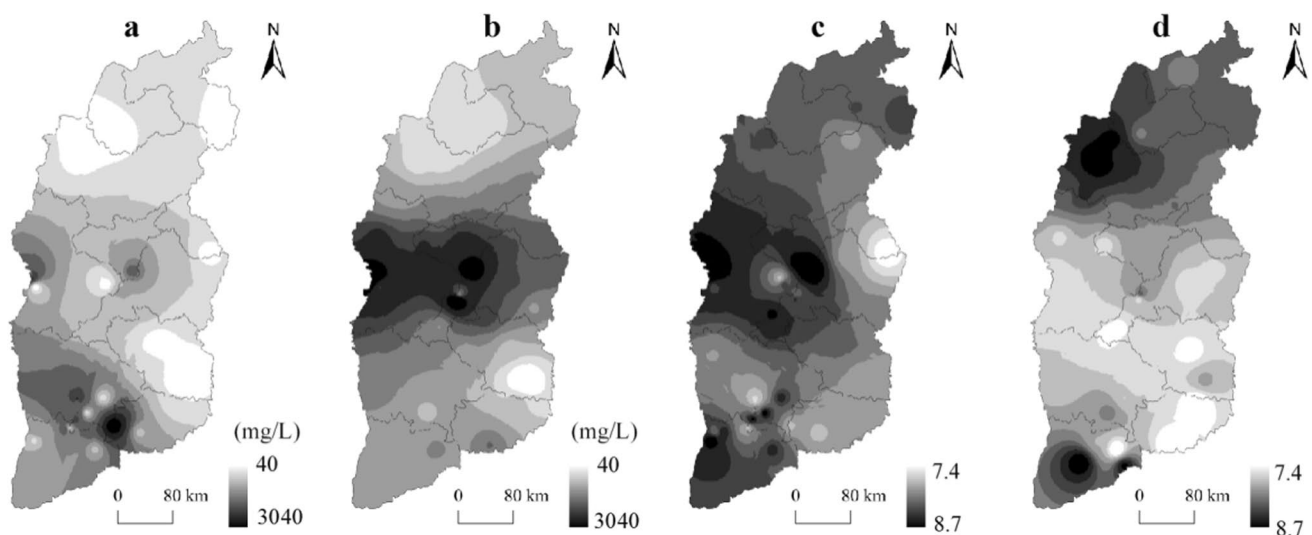

Fig. 2 Spatial distributions of shallow groundwater pH and TDS in the study area during different seasons. **a**. Slowflow season TDS; **b**. Quickflow season TDS; **c**. Slowflow season pH; **d**. Quickflow season pH

slowflow season, the spatial variations of the groundwater TDS are not obvious. On the contrary, pronounced variations of the groundwater TDS appeared in the quickflow season, where the highest TDS concentration was observed on the central region and lower TDS values appeared in the northern and southern Shanxi Province.

Figure 3 shows the spatial distribution of main ion concentrations during the study period. In the slowflow season, the spatial variation pattern of average Na^+ concentration is completely different from other dissolved cations. The higher Na^+ values were mainly distributed in the Taiyuan Basin, the Yuncheng Basin, and Lvliang Mountains. Relative lower values were observed in the northern Shanxi and the Changzhi Basin. The spatial distribution of K^+, Mg^{2+}, and Ca^{2+} values were similar in the slowflow season, where the higher values appeared in the southern Shanxi. In the quickflow season, the spatial variations of major cations had remarkable different patterns. Higher Na^+ and Mg^{2+} values were mainly distributed in the Taiyuan Basin. The concentrations of Ca^{2+} and K^+ of the southern Shanxi province are higher than other regions.

(S: Slowflow season, Q: Quickflow season).

As for the groundwater anions, the significance of spatial variation during the slowflow season follows descending order: $Cl^- > SO_4^{2-} > HCO_3^-$. In the slowflow season, the higher concentration of anions are mostly concentrated in the southern part of the study area and the Lvliang Mountains (Cl^- values). In the quickflow season, the spatial variation pattern of anion concentration is different from the slowflow season. The higher values of anion concentration (Cl^-, SO_4^{2-}, and $HCO3^-$) most concentrated in the middle part. As for major ions, Na^+ and Mg^+ showed the similar seasonal and spatial distributions with the Cl^- and SO_4^{2-}, respectively, which indicates the Na^+ and Mg^+ are associated with the Cl^- and SO_4^{2-}.

In this study, we classified the groundwater samples into categories according to season in order to better investigate the seasonal distribution of groundwater major ions. The higher TDS concentration appeared in the quickflow season and the lower TDS concentration was observed in the slowflow season. The highest concentration of most crustal ions (Na^+, K^+, Cl^-, and NO_3^-) were observed in the quickflow season due to the large input of dust accumulated in the summer monsoon. Ion concentrations decreased in the slowflow season because of the precipitation reduction. The relative higher concentration in Na^+ and Cl^- mainly due to the salinity input. In the quickflow season a consequence of flushing of saline soil horizons, reaching the underground aquifer during summer periods via the infiltration of the aeration zone. The concentration of some ions (Ca^+, HCO_3^-, and SO_4^{2-}) slightly decreased from the slowflow season to the quickflow season, mostly due to high irrigation rates and flushing of accumulated silicates (NaCl) developed in soils and the dissolution of carbonate and sulphate minerals is inhibited.

Temporal and spatial variations of groundwater stable isotope

δ^2H and $\delta^{18}O$ of groundwater samples ranged from -86.26‰ to -57.02‰ with a mean value of -70.78‰ and from -11.52‰ to -8.39‰ with a mean value of -9.28‰, respectively. For the slowflow season, δ^2H values of groundwater varied from -86.26‰ to -57.02‰ with a mean value of -69.57‰ and from -11.52‰ to -9.20‰ with a mean value of -8.98‰ for $\delta^{18}O$, respectively. For the quickflow season, the groundwater δ^2H ranged from -86.23‰ to -58.35‰ with a mean value of -72.00‰ and from -11.48‰ to -8.39‰ with a mean value of -9.59‰ for $\delta^{18}O$, respectively.

The groundwater samples in study area have obviously spatial variation in stable isotopic composition. As shown in Fig. 4, the δ^2H and $\delta^{18}O$ values increase gradually from the middle part to the northern and southern part, where significant higher δ^2H and $\delta^{18}O$ values appeared in the northern plateau and Changzhi Basin. Lower values of δ^2H and $\delta^{18}O$ in groundwater appeared in the Taiyuan Basin.

Compare with two sampling seasons, the groundwater δ^2H and $\delta^{18}O$ in the quickflow season have relatively lower value than that of the slowflow season. The probability reason is that the groundwater in the quickflow season was affected by the precipitation. In the quickflow season, the δ^2H and $\delta^{18}O$ enrichment areas (southern part) have expanded. However, the areas of lower δ^2H and $\delta^{18}O$ values appearing in the middle part of study area presented reduce trend. The relatively significant seasonal variations of groundwater δ^2H and $\delta^{18}O$ indicate the groundwater has different composition patterns during the two observation periods.

Hydrochemical types

Piper ternary diagrams can present the importance of different weathering regimes by providing a way to visualize the composition and water types of different water (Jiang et al. 2015). In our study, we projected all the groundwater samples collected from the Shanxi Province during the study period in the Piper diagram (Fig. 5).

In the slowflow season, the piper diagram shows that most samples are carbonate type water, whereas no chloride-type water samples are identified. In the cation diagram, the samples are mainly located on the lower-left corner and lower-right corner, and the dominant cations are Ca^{2+} and Na^+. In the anion diagram, two sample data clusters can be observed. Many water samples locate on the lower-left corner, and carbonic acid is the dominant ion. The other sample points locate on the upper-left corner. SO_4^{2-} ($CO_3^{2-} + HCO_3^- = 1:1$) is on the middle line, which indicates these samples are dominated by sulfuric acid. None of the samples are chlorine type. In the slowflow

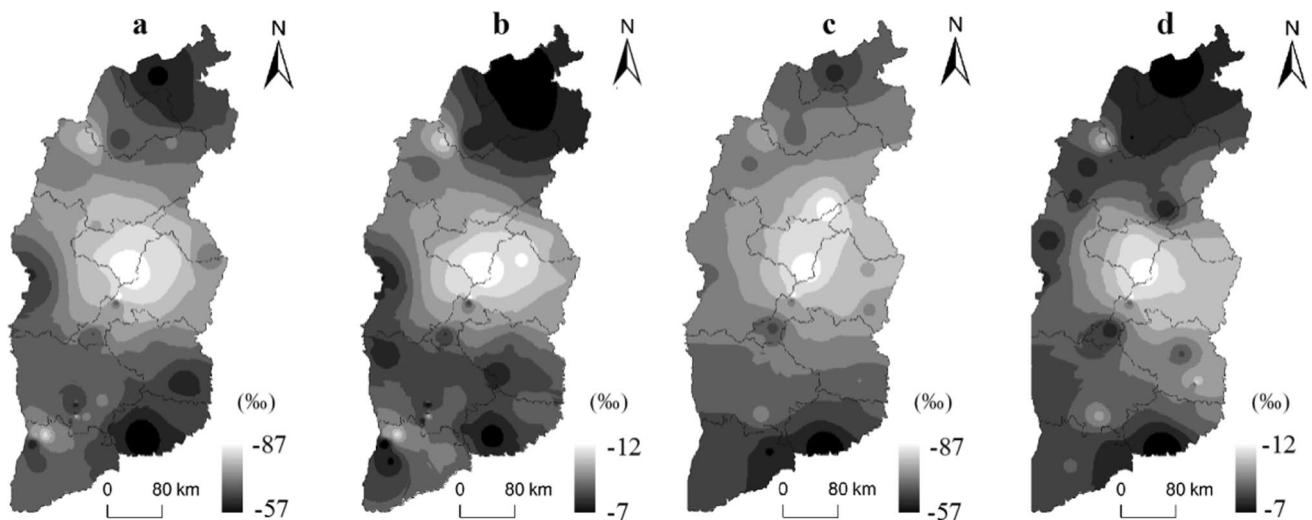**Fig. 3** Main ion spatial distribution characteristics of different seasons in the study area
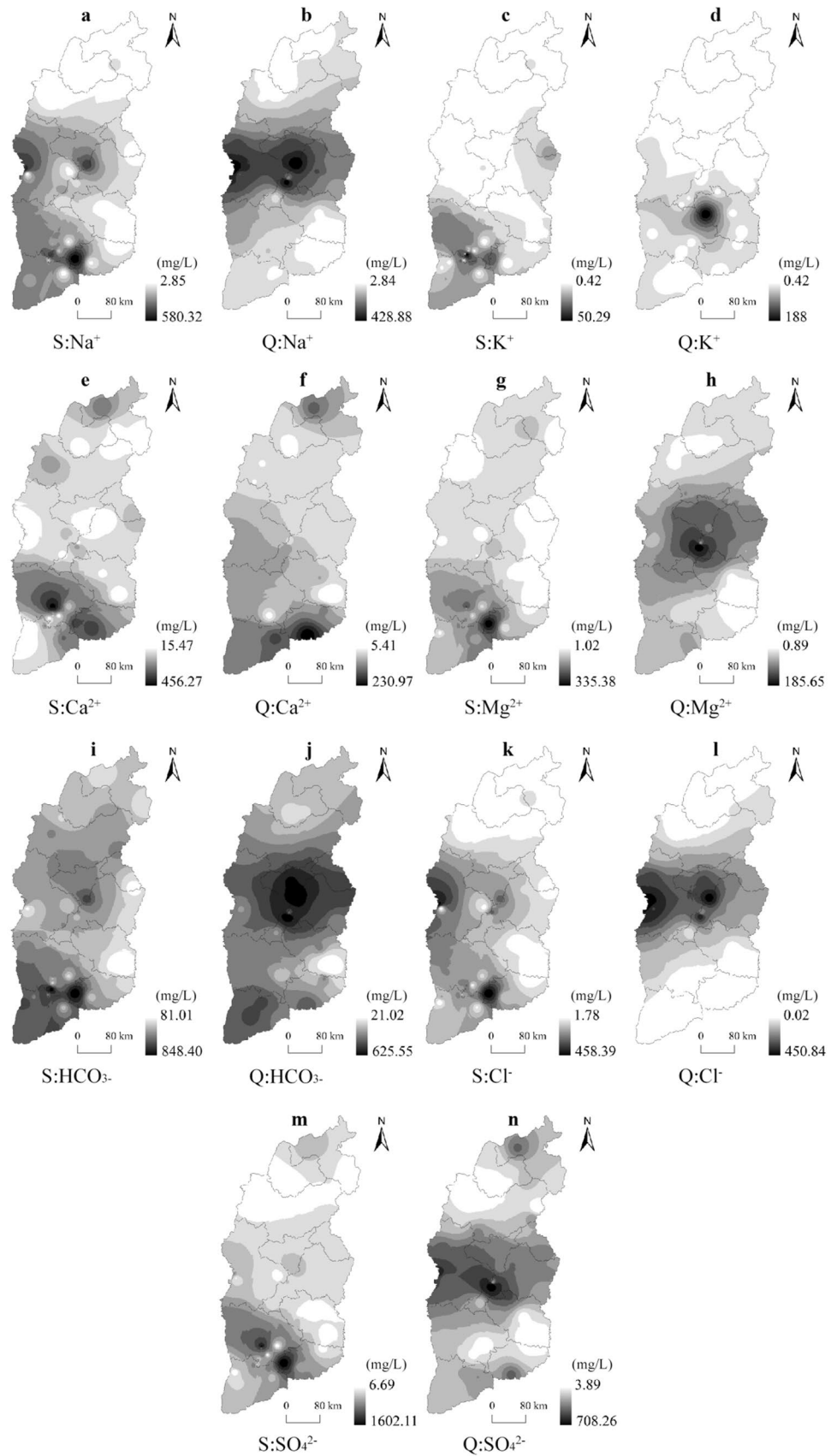
Fig. 4 δ^2H and $\delta^{18}O$ spatial distribution characteristics of different seasons in the study area. **a**. Slowflow season δ^2H; **b**. Slowflow season $\delta^{18}O$; **c**. Quickflow season δ^2H; **d**. Quickflow season $\delta^{18}O$
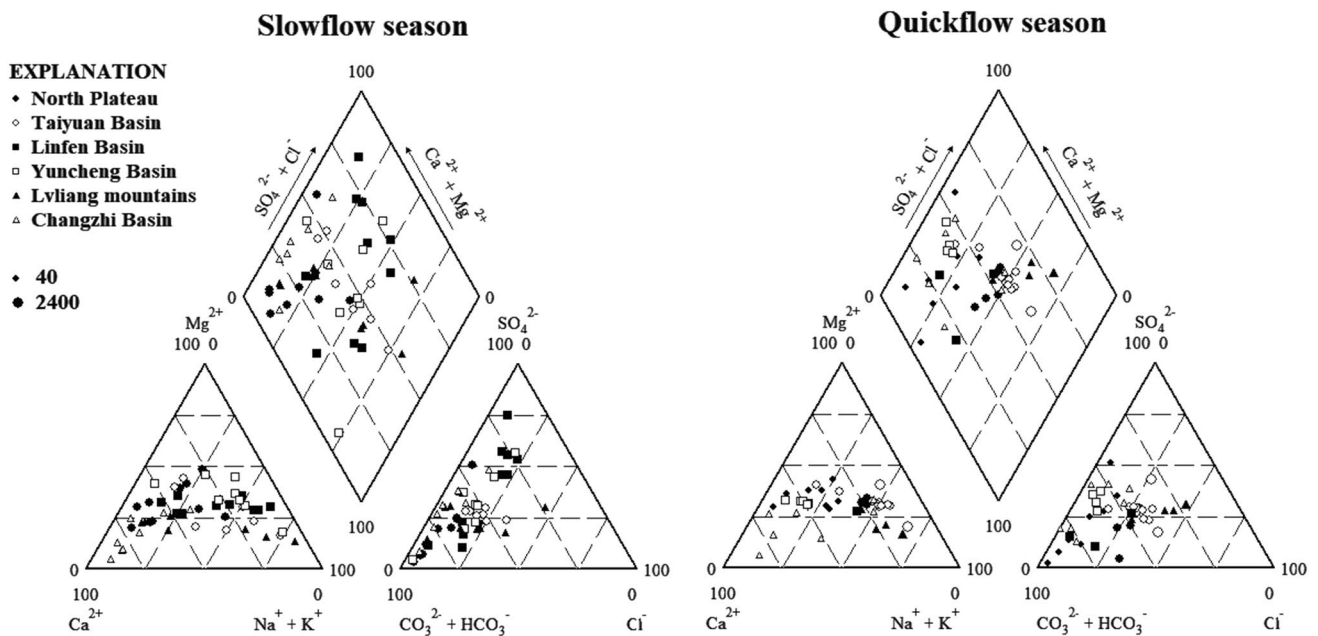

Fig. 5 Piper diagram of cations and anions in groundwater in Shanxi

season, the groundwater samples mainly belong to the (HCO_3^--Ca^{2+}-Na^+) type and the (HCO_3^--SO_4^{2-}-Ca^{2+}-Na^+) type, which shows relative HCO_3^-, SO_4^{2-}, Ca^{2+}, and Na^+ enrichments. A few groundwater samples collected from the Linfen Basin belong to the (SO_4^{2-}-Ca^{2+}) type. The (HCO_3^--Mg^{2+}) water type can be observed in the groundwater samples from the Lvliang Mountains (Table 2).

In the slowflow season, the Piper diagram shows that most samples belong to the carbonate type water, whereas a

few water samples collected from the Lvliang Mountains are the chloride-type. In the cation diagram, majority samples are located on the lower part, and the dominant cations are Na^+, K^+, and Ca^{2+}. There are a large of groundwater samples distributed at the lower-left corner in the anion diagram indicating that carbonate acid is the main anion for these samples (Fig. 5).

In the quickflow season, the groundwater samples also mainly belong to the (HCO_3^--Ca^{2+}-Na^+) type and the

Table 2 Geochemical Types of Shallow Groundwater in Shanxi Province

	Slowflow season (TDS mg·L^{-1})	Quickflow season (TDS mg·L^{-1})	Slowflow season	Quickflow season
North Plateau	608	698	$HCO_3^--Ca^{2+}$ $HCO_3^--Ca^{2+}-Mg^{2+}-Na^+$ $HCO_3^--SO_4^{2-}-Ca^{2+}$	$HCO_3^--Ca^{2+}$ $HCO_3^--Ca^{2+}-Na^+$
Taiyuan Basin	1 004	1 432	$HCO_3^--Mg^{2+}$ $HCO_3^--SO_4^{2-}-Na^+$ $HCO_3^--SO_4^{2-}-Ca^{2+}-Na^+$ $HCO_3^--SO_4^{2-}-Ca^{2+}-Mg^{2+}-Na^+$	$HCO_3^+-Na^+$ $HCO_3^--SO_4^{2-}-Na^+$ $HCO_3^--SO_4^{2-}-Ca^{2+}-$ $Mg^{2+}-Na^+$ $HCO_3^--Cl^--Na^+$
Linfen Basin	1 298	852	$SO_4^{2-}-Ca^{2+}$ $HCO_3^--Ca^{2+}-Na^+$ $HCO_3^--Mg^{2+}-Na^+$	$HCO_3^--Ca^{2+}-Na^+$ $HCO_3^--SO_4^{2-}-$ $Ca^{2+}-Na^+$
Yuncheng Basin	1 272	940	$HCO_3^--Na^+$ $HCO_3^--SO_4^{2-}-Na^+$ $HCO^--SO_4^{2-}-Mg^{2+}-Na^+$	$HCO_3^--Ca^{2+}$ $HCO_3^--SO_4^{2-}-Ca^+$
Lvliang mountains	835	1 569	$CO_3^--Ca^{2+}$ $HCO_3^--Mg^{2+}$ $HCO_3-Ca^{2+}-Na^+$ $HCO_3^--SO_4^{2-}Ca^{2+}-Mg^{2+}$	$HCO_3^--Ca^{2+}-Na$ $HCO_3^--Cl^--Na^+$ $HCO_3^--SO_4^{2-}-Cl^--Na^+$
Changzhi Basin	513	737	$HCO_3^--Ca^{2+}$ $HCO_3^--SO_4^{2-}-Ca^{2+}-Na^+$ $HCO_3^--SO_4^{2-}-Ca^{2+}$	$HCO_3^--Ca^{2+}$ $HCO_3^--Ca^{2+}-Na^+$ $HCO_3^--SO_4^{2-}-Ca^{2+}$

($HCO_3^--SO_4^{2-}-Ca^{2+}-Na^+$) type. Unique groundwater types are observed in the Taiyuan Basin and the Lvliang Mountains. In the two regions, the groundwater shows the hydrochemical evolution from the ($HCO_3^--Ca^{2+}-Na^+$) type, to the ($HCO_3^--SO_4^{2-}-Ca^{2+}-Na^+$) type, to the ($HCO_3^--Cl^--Na^+$) type, which depicts a relative Cl enrichment (Table 2).

Factors controlling water geochemistry

The hydrochemical characteristic of groundwater is associated with the types of recharge sources and their chemical properties (Pu et al. 2013b; Jiang et al. 2015). Rock dominance, atmospheric precipitation, and evaporation-crystallization processes are considered to three major end-members which controlled the chemical processes of groundwater based on the analyses of numerous water samples with different types to elaborate the controlling patterns of world water chemistry by Gibbs (1970) and Yang et al. (2018). The modified Gibbs scheme diagrams was defined by the variations of ionic $Na^+/(Na^++Ca^{2+})$ and $SO_4^{2-}/(SO_4^{2-}+HCO_3^-)$ ratios as a function of TDS. Groundwater hydrochemical data in the study area was plotted in the Gibbs diagram (Fig. 6).

As Fig. 6 shown, most of groundwater samples are located in the controlling region of rock dominance, and deviated from the region of atmospheric precipitation, which indicated that the rock weathering is the main controlling factor for the hydrochemical process of groundwater in both seasons.

In the Gibbs diagram (Fig. 6), there are only two groundwater samples (from the Yuncheng Basin) located in the transitional band of the rock weathering and the precipitation dominance, which indicates that the precipitation has a significant influence on the groundwater in the southern Shanxi province. In addition, some groundwater samples from the Lvliang Mountains and the Linfen Basin are characterized by high ratios of $Na^+/(Na^++Ca^{2+})$ and $Cl^-/(Cl^-+HCO_3^-)$ and medium concentration of TDS. These samples are unobvious affected by the rock weathering and evaporation crystallization. Human activities such as coal exploitation and well-developed irrigation agriculture may were the main reason for this phenomenon.

Discussions

The effect of lithology for the groundwater

According to the results of the Gibbs diagram, the main controlling factor of hydrochemical characteristic of groundwater in study area is the rock weathering. Determination of the chemical composition of groundwater can effectively improve the understanding of tracing the weathering processes of the groundwater. The source of groundwater ions was applied to decide by the ratio of Ca^{2+}/Na^+, Mg^{2+}/Na^+, and HCO_3^-/Na^+ (Gaillardet et al. 1999; Yang et al. 2018).

Fig. 6 Plots of the major ions of groundwater within the Gibbs boomerang envelope in Shanxi. (**a**) Slowflow season. (**b**) Quick-flow season
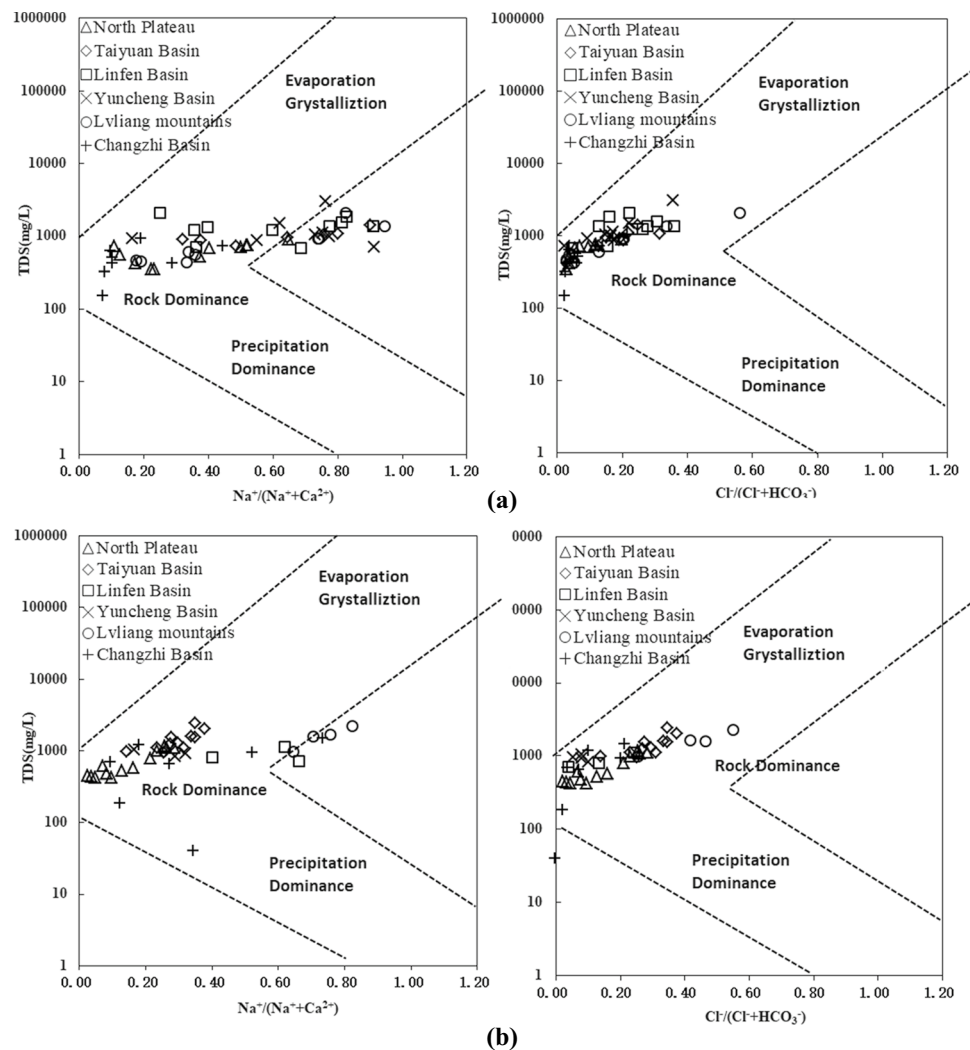
In the slowflow season, majority of the groundwater sample points were mainly derived from the silicate weathering, which had relatively lower ratios of Ca^{2+}/Na^+ and Mg^+/Na^+, Ca^{2+}/Na^+ and HCO_3^-/Na^+. A number of samples located on the lower-left corner, so the evaporation has important effects on the ion content of groundwater. Few groundwater samples were influenced by the carbonate weathering. However, in the quickflow season, the ratios of Ca^{2+}/Na^+ and Mg^+/Na^+, Ca^{2+}/Na^+ and HCO_3^-/Na^+ had similar distribution patterns to the slowflow season. Based on Fig. 7, the chemical compositions of the groundwater sources in study area were mainly influenced by the dissolution of silicates and evaporation.

The influence of human activities for the groundwater

Pollutants produced by human activities usually spread to surface water through sewage discharge and then infiltrate into groundwater system through surface water-groundwater interaction (Li et al. 2007a, b; Yang et al. 2018). Residual fertilizers in the agricultural irrigation and pollution in the industrial activities are defined as important sources of pollution for groundwater system (Wright et al. 2011; Yang et al. 2018). In recent years, large-scale cultivation of crops and sharp decrease of surface water resources in study area made the agricultural irrigation increasingly relying on groundwater, which has resulted in serious depletion of groundwater and nitrate contamination (Xing et al, 2013). Assessing the sustainability of irrigated systems urgently need to improve the understanding of the relationship between groundwater resource and nitrate concentration. In general, NO_3^- and SO_4^{2-} are sensitive ion components for regional groundwater pollution, which are easily obviously affected by human activities, can be used to distinguish the input characteristics of human activities on water quality (Pu et al. 2013a&b; Han et al. 2014). In agricultural activities, the NO_3^- content increasing usually caused by the application of nitrogen fertilizers, whereas the SO_4^{2-} mainly
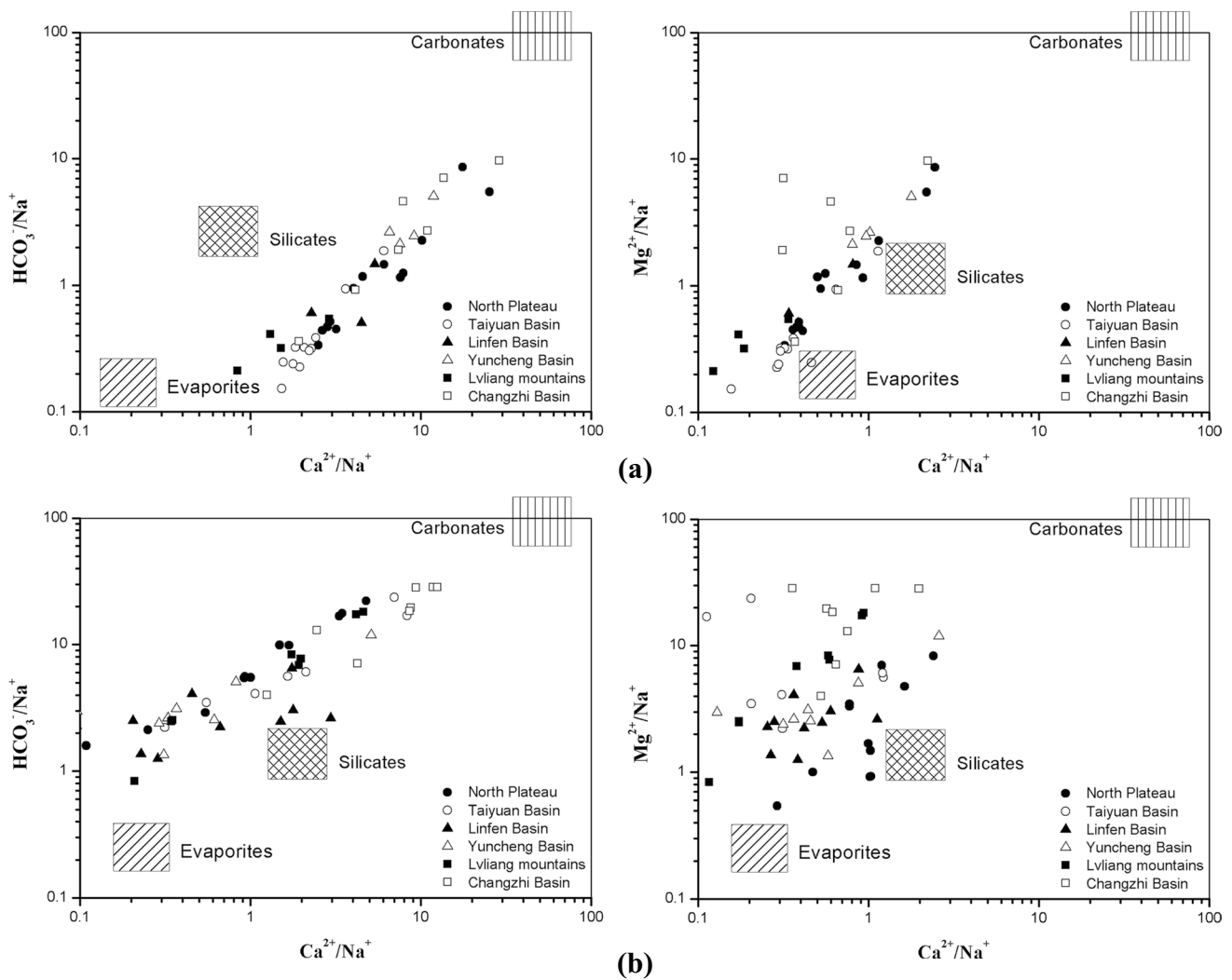
Fig. 7 Plots of HCO_3^-/Na^+ versus Ca^{2+}/Na^+ and Mg^{2+}/Na^+ versus Ca^{2+}/Na^+ ratios. (**a**) Slowflow season. (**b**) Quickflow season

originates from atmospheric deposition and industrial activities (Han et al. 2014). In this paper, to study the effects of human activities on the ionic characteristics in groundwater of the study area, we selected the ratio of NO_3^- to SO_4^{2-} and of Cl^- to Na^+ as indicators for the distinction between rock weathering and anthropogenic sources to the groundwater ion sources during study periods (Fig. 8).

The ratio of SO_4^{2-} to Na^+ in most groundwater samples was higher than 0.5 (Fig. 8), which indicated that content of SO_4^{2-} of most groundwater samples were influenced by human activities during two study periods. This finding was especially pronounced for the groundwater samples in the quickflow season, where the ratio reached 1. NO_3^-/Na^+ ratio was higher than 0.5 for most groundwater samples in the study area, indicating more anthropogenic inputs to groundwater. The ratios of NO_3^- to Na^+ for some groundwater samples collected from the Yuncheng Basin, Linfen Basin, and Changzhi Basin were greater than 4, which indicated

that NO_3^- in the groundwater were influenced by human activities such as fertilization. In study area, most farmland distributed in the inner valley with lots of agricultural irrigation systems. The higher NO_3^- content was observed in the inner valley such as the Yuncheng Basin, Linfen Basin, and Changzhi Basin, which may contributed to agriculture irrigation activities.

The influence of surface water-groundwater interaction for the groundwater

As important components of the hydrological system, the interaction between surface water and groundwater appeared in various topographic and climatic landscapes. It is necessary to understanding the mechanism of interaction between groundwater and surface water in order to manage water resources effectively (Sophocleous 2001; Allen et al. 2010; Klaus and Mcdonnell, 2013; Zhang et al. 2016a, b; Kebede
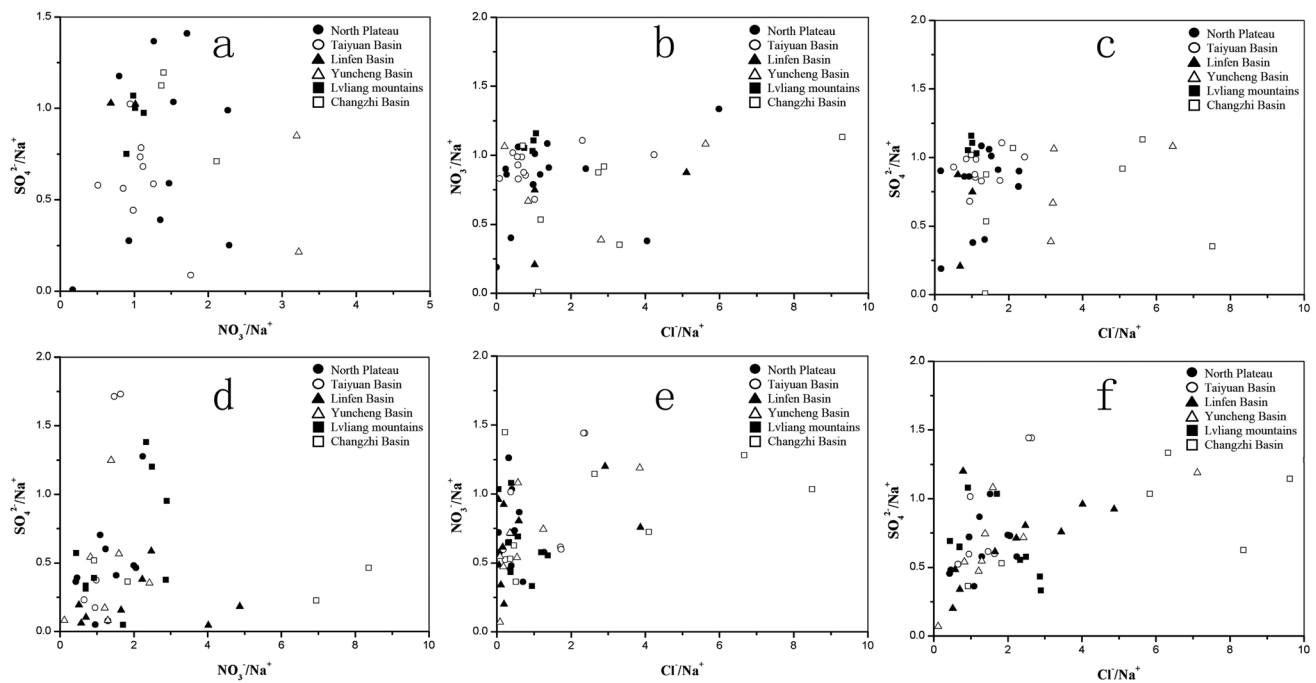
Fig. 8 Relationships among some ions in groundwater of Shanxi. Slowflow season **a**-**c**; Quickflow season **e**–**f**

et al. 2017; Wang et al. 2018). The valley in the central part of the Shanxi Province is a concentrated region of cultivated land, population and cities. The transition exploitation of groundwater resources in valley basin caused by large-scale agricultural activities and increasing water demand of production and living has resulted in the transformation between surface water and groundwater became complex. In this study, we selected 17 typical groundwater samples located in the central basin of Shanxi Province (Taiyuan basin:TG1-TG7, Linfen basin: LG1-LG4, Yuncheng basin: YG1-YG6) to analyze the influence of surface water on groundwater environment.

According to the EMMA method (Fig. 9), the groundwater samples of the Taiyuan basin, Linfen basin and Yuncheng basin during the slowflow season were plotted away from the river water samples and precipitation samples, which indicated the interaction between groundwater and surface water (river water and precipitation) is not obvious. In quickflow period, there are some groundwater samples of the Taiyuan basin was located nearby the groundwater samples of the slowflow season and surface river water, which indicated that groundwater samples may be affected by groundwater samples in slowflow and surface river water. As for the Linfen basin, most groundwater samples points in quickflow season were plotted in the triangle composed of the average values of tracer TDS and δ18O of the groundwater in the slowflow season, river water and precipitation,

which indicated that significant transformation relationship between the groundwater in the quickflow season and surface water (precipitation and river water) in the Linfen basin. Significant spatial and temporal variations in the concentrations of TDS and $\delta^{18}O$ can be observed in different water samples of the Yuncheng basin. The location of these samples suggested the interaction relationship between groundwater and surface water of the Yuncheng basin is complex. However, there are still some groundwater samples fall into the triangle that is spanned by three end members (precipitation, groundwater in slowflow period, and river water), which suggested that the streamflow is also a mixture of these three end members.

According to the results of three-component method, there are four sampling points in the Taiyuan basin shown that the groundwater in the quickflow season has been obviously influenced by the river water and precipitation, and three sampling points have not significant interaction relationship between groundwater and surface water. At TG3 and TG5 points, the contribution of surface river water recharge groundwater is more than 44%, while significant contribution of precipitation supply to groundwater can be observed at TG1 and TG7 (Fig. 10). Groundwater of the slowflow season and river water is mainly recharge sources for the groundwater in quickflow season. In the Linfen basin, the transformation between surface water and groundwater during the quickflow season is obvious. The contribution

Fig. 9 Groundwater observation and the values of tracers TDS and $\delta^{18}O$ of the end members (river water and precipitation)
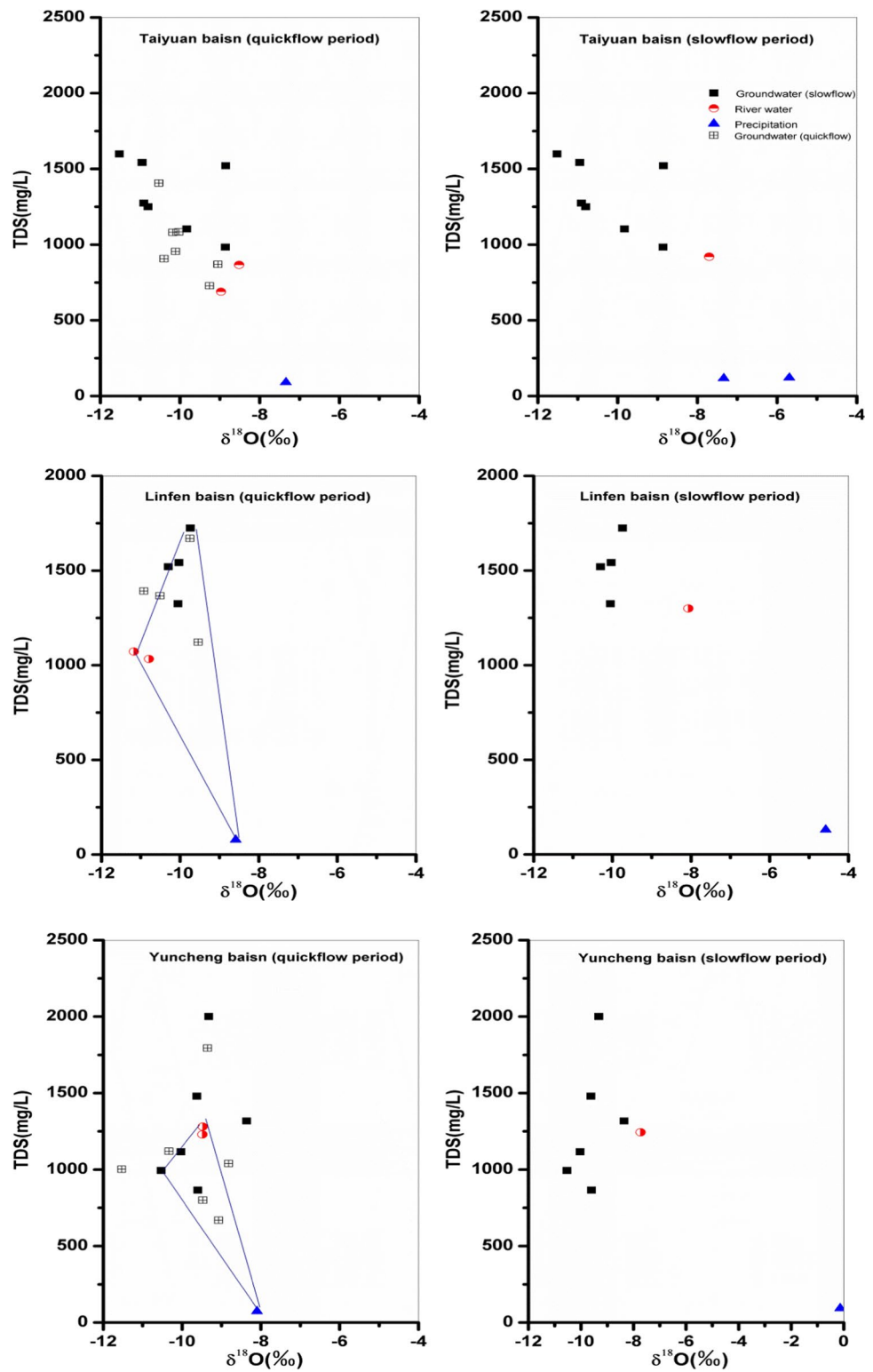
rate of surface river water recharges the groundwater shown a gradually increasing trend from the northern part to the southern part of the Linfen basin, which is similar to the streamflow direction of the Fenhe river.

In the Yuncheng basin, the transformation between surface water and groundwater is complicated during the quickflow season. There are three samples (YG1, YG4 and YG6) of groundwater in the quickflow season were contributed by
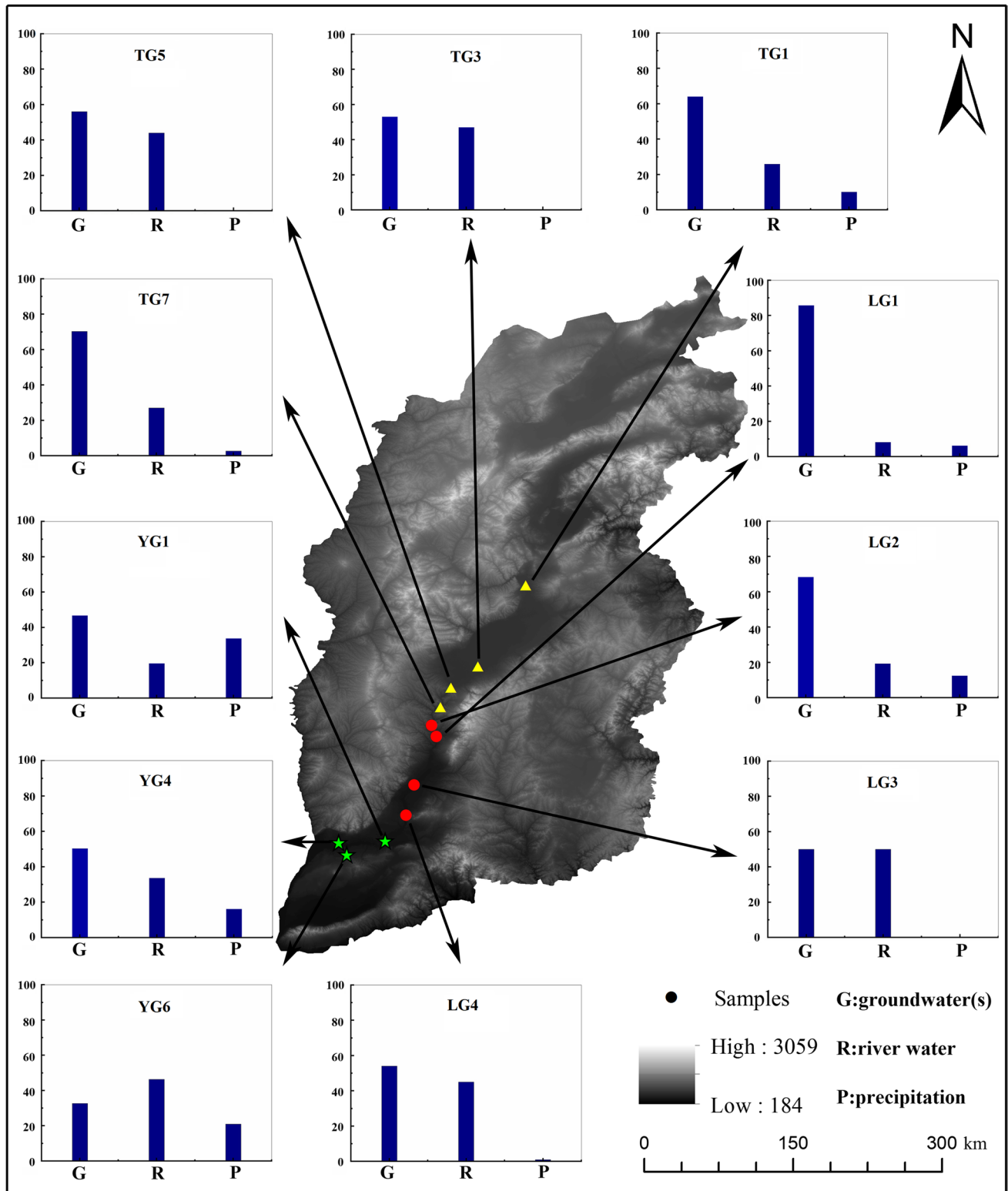
Fig. 10 Contributions of groundwater in the slowflow season, river water and precipitation to groundwater in the quickflow season in the Taiyuan basin, Linfen basin and Yuncheng basin

precipitation and surface river water. The larger contribution rate of surface river water to groundwater are observed at YG4 (33.6%) and YG6 (46.4%) point, while at YG1 point, the contribution rate of precipitation recharge to groundwater (33.7%) is larger than that of surface river water (19.6%). At YG2 and YG3, the surface river water was proved to receive the groundwater recharge during the quickflow season. Compare with three study region, river water has larger contribution to the groundwater of the Taiyuan basin and precipitation has a larger influence on the groundwater of the Yuncheng basin.

Conclusions

In this study, groundwater samples were mildly alkaline. HCO_3^- and Na^+ dominated the total mass of the anions and cations respectively. During the slowflow season, the main ion content of groundwater samples was in the following descending order: $HCO_3^- > SO_4^{2-} > Na^+ > Ca^{2+} > Cl^- > Mg^{2+} > K^+$ (contents are 355.09, 208.29, 114.93, 83.92, 79.19, 47.62, 3.84 mg·L^{-1}). In the quickflow season, the main ion content of groundwater samples was in the following descending order: $HCO_3^- > SO_4^{2-} > Na^+ > Cl^- > Ca^{2+} > Mg^{2+} > K^+$ (contents are 345.23, 161.78, 123.82, 111.00, 77.32, 47.65, 6.42 mg·L^{-1}).

Significant seasonal and spatial variations can be observed in TDS, δ^2H, and $\delta^{18}O$ of groundwater samples. More pronounced variations of groundwater TDS appeared in the quickflow season, where the highest TDS concentration was observed in the central region and lower TDS values appeared in the northern and southern part of the study area. The higher TDS concentration appeared in the quickflow season and lower TDS concentration was observed in the slowflow season. The δ^2H and $\delta^{18}O$ increased gradually from the middle part to the northern and southern parts respectively, where significant higher δ^2H and $\delta^{18}O$ values occurred in the north plateau and Changzhi Basin. Lower values of δ^2H and $\delta^{18}O$ in groundwater appeared in the Taiyuan Basin.

The groundwater samples mainly belong to the (HCO_3^--Ca^{2+}-Na^+) type and the (HCO_3^--SO_4^{2-}-Ca^{2+}-Na^+) type. The chemical composition of the groundwater in the study area is significantly influenced by rock weathering during the study periods. Some groundwater samples from the Lvliang Mountains and the Linfen Basin are influenced by the human activities.

The chemical compositions of the groundwater sources were mainly affected by the dissolution of silicates and evaporation. Some groundwater samples collected from the Yuncheng Basin, Linfen Basin, and Changzhi basin were affected by human activities such as fertilization. The significant influence of surface water-groundwater interaction for the groundwater can be observed at the valley basin in the central part. The interaction between surface water and groundwater in the Linfen basin is especially remarkable and its contribution rate of surface river water recharge the groundwater shown a gradually increasing trend from the northern part to the southern part.

References

Allen DJ, Darling WG, Gooddy DC, Lapworth DJ, Newell AJ, Williams AT, AllenI D, Abesser C (2010) Nteraction between groundwater, the hyporheic zone and a Chalk stream: a case study from the River Lambourn, UK. Hydrogeol J 18:1125–1141

Barbecot F, Marlin C, Gibert E, Dever L (2000) Hydrochemical and isotopic characterisation of the Bathonian and Bajocian coastal aquifer of the Caen area (northern France). Appl Geochem 15:791–805

Batabyal AK (2017) Hydrogeochemical processes and contaminants enrichment with special emphasis on fluoride in groundwater of Birbhum district, West Bengal, India. Environ Earth Sci 76:285

Brindha K, Elango L (2011) Hydrochemical characteristics of groundwater for domestic and irrigation purposes in Madhuranthakam, Tamil Nadu, India. Earth Sci Res J 15:101–108

Dogramaci S, Skrzypek G, Dodson W, Grierson PF (2012) Stable isotope and hydrochemical evolution of groundwater in the semi-arid Hamersley Basin of sub-tropical northwest Australia. J Hydrol 475:281–293

Gaillardet J, Dupré B, Louvat P, Allègre CJ (1999) Global silicate weathering and CO_2, consumption rates deduced from the chemistry of large rivers. Chem Geol 159:3–30

Gibbs RJ (1970) Mechanisms controlling world water chemistry. Science 170:1088–1090

Han D, Kohfahl C, Song X, Xiao G, Yang J (2011) Geochemical and isotopic evidence for palaeo-seawater intrusion into the south coast aquifer of Laizhou Bay, China. Appl Geochem 26:863–883

Han D, Tong X, Currell MJ, Cao G, Jin M, Tong C (2014) Evaluation of the impact of an uncontrolled landfill on surrounding groundwater quality, Zhoukou, China. J Geochem Explor 136:24–39

Hu S, Luo T, Jing C (2013) Principal component analysis of fluoride geochemistry of groundwater in Shanxi and Inner Mongolia, China. J Geochem Explor 135(6):124–129

Jiang L, Yao Z, Liu Z, Wang R, Wu S (2015) Hydrochemistry and its controlling factors of rivers in the source region of the Yangtze River on the Tibetan plateau. J Geochem Explor 155:76–83

Karmegam U, Chidambaram S, Prasanna MV, Sasidhar P, Manikandan S, Johnsonbabu G, Dheivanayaki V, Paramaguru P, Manivannan R, Srinivasamoorthy K, Anandhan P (2011) A study on the mixing proportion in groundwater samples by using Piper diagram and Phreeqc model. Acta Geochemical 30:490

Kattan Z (2015) Chemical and isotopic characteristics of the Euphrates River water, Syria: factors controlling its geochemistry. Environ Earth Sci 73:4763–4778

Kattan Z (2018) Using hydrochemistry and environmental isotopes in the assessment of groundwater quality in the Euphrates alluvial aquifer. Syria Environ Earth Sci 77:45

Kebede S, Abdalla O, Sefelnasr A, Tindimugaya C, Mustafa O (2017) Interaction of surface water and groundwater in the Nile River basin: isotopic and piezometric evidence. Hydrogeol J 25:707–726

Klaus J, Mcdonnell JJ (2013) Hydrograph separation using stable isotopes: Review and evaluation. J Hydrol 505:47–64

Kumar PJS, James EJ (2013) Physicochemical parameters and their sources in groundwater in the Thirupathur region, Tamil Nadu, South India. Appl Water Sci 3:219–228

Kumar A, Singh CK (2015) Characterization of Hydrogeochemical Processes and Fluoride Enrichment in Groundwater of South-Western Punjab. Water Qual Expo Health 7:373–387

Li C, Kang S, Zhang Q, Kaspari S (2007) Major ionic composition of precipitation in the Nam Co region, Central Tibetan Plateau. Atmos Res 85:351–360

Li T, Ji H, Jiang Y, Wang L (2007) Hydro-geochemistry and the sources of DIC in the upriver tributaries of the Ganjiang River. Acta Geogr Sin 20:257–271

Li P, Qian H, Wu J (2011) Hydrochemical Characteristics and Evolution Laws of Drinking Groundwater in Pengyang County, Ningxia, Northwest China. J Chem 8:565–575

Liu X, Liu J, Feng X (2016) Study on the Marine Sedimentary Environment Evolution of the Southern Laizhou Bay under the Impact of Port Projects. J Ocean Univ China 15:553–560

Pu T, He Y, Zhang T, Wu J, Zhu G, Li C (2013) Isotopic and geochemical evolution of ground and river waters in a karst dominated geological setting: a case study from Lijiang Basin, South Asia monsoon region. Appl Geochem 33:199–212

Pu T, He Y, Zhu G, Zhang N, Du J, Wang C (2013) Characteristics of water stable isotopes and hydrograph separation in Baishui catchment during the wet season in Mt. Yulong region, south western China. Hydrol Process 27:3641–3648

Samake M, Tang Z, Hlaing W, Ndoh Mbue I, Kasereka K, Balogun WO (2011) Groundwater Vulnerability Assessment in Shallow Aquifer in Linfen Basin, Shanxi Province, China Using DRASTIC Model. Res J Appl Sci 4:616–622

Sophocleous M (2001) Interactions between groundwater and surface water: the state of the science. Hydrogeol J 10:348–348

Stober I (2014) Hydrochemical properties of deep carbonate aquifers in the SW German Molasse basin. Geothermal Energy 2:13

Sun Y, Zhang A, Wang Q, Yi H, Liu Y, Tian Q (2011) Influences of Human Activities on the Coastal Landform and Sea Water Invasion Along the Southern Laizhou Bay during the Past 30 Years. Mar Geol Q Geol 31:43–50

Sun C, Li X, Chen Y, Li W, Stotler RT, Zhang Y (2016) Spatial and temporal characteristics of stable isotopes in the Tarim River Basin. Isot Environ Health Stud 52:1

Sun C, Yang J, Chen Y, Li X, Yang Y, Zhang Y (2016) Comparative study of streamflow components in two inland rivers in the Tianshan Mountains, Northwest China. Environ Earth Sci 75:1–14

Sun Z, Song X, Bu H, Yang L, Ma Y, Zhang Y, Han D (2016) Origin of groundwater salinity and hydrochemical processes in an unconfined aquifer: case of Yang-Dai River basin in Qinhuangdao (China). Environ Earth Sci 75:1–12

Sun C, Li X, Chen W, Chen Y (2017) Climate change and runoff response based on isotope analysis in an arid mountain watershed of the western Kunlun Mountains. Hydrol Sci J 62:319–330

Sun C, Shen Y, Chen Y, Chen W, Liu W, Zhang Y (2018) Quantitative evaluation of the rainfall influence on streamflow in an inland mountainous river basin within Central Asia. Hydrol Sci J 63:17–30

Sung KY, Yun ST, Park ME, Koh YK, Choi BY, Hutcheon L, Kim KH (2012) Reaction path modeling of hydrogeochemical evolution of groundwater in granitic bedrocks, South Korea. J Geochem Explor 118:90–97

Tang Q, Xu Q, Zhang F, Huang Y, Liu J, Wang X, Yang Y, Liu X (2013) Geochemistry of iodine-rich groundwater in the Taiyuan Basin of central Shanxi Province, North China. J Geochem Explor 135:117–123

Wang P, Song X, Han D, Zhang Y, Liu X (2010) A study of root water uptake of crops indicated by hydrogen and oxygen stable isotopes: A case in Shanxi Province, China. Agric Water Manag 97:475–482

Wang S, Yuan R, Tang C, Song X, Currell M, Yang Z, Sheng Z (2018) Combination of CFCs and stable isotopes to characterize the mechanism of surface water-groundwater interaction in a headwater basin of the North China Plain. Hydrol Process 32:1571–1587

Wright IA, Davies PJ, Findlay SJ, Jonasson OJ (2011) A new type of water pollution: concrete drainage infrastructure and geochemical contamination of waters. Mar Freshw Res 62:1355–1361

Xing L, Guo H, Zhan Y (2013) Groundwater hydrochemical characteristics and processes along flow paths in the North China Plain. J Asian Earth Sci 70–71:250–264

Yang L, Zhu G, Shi P, Li J, Liu Y, Tong H, Hu P, Liang F, Pan H, Guo H, Zhang Y (2018) Spatiotemporal characteristics of hydrochemistry in Asian arid inland basin-a case study of Shiyang River Basin. Environ Sci Pollut Res 25:2293–2302

Zhang J, Tsujimura M, Song X, Sakakibara K (2016) Using stable isotopes and major ions to investigate the interaction between shallow and deep groundwater in Baiyangdian Lake Watershed, North China Plain. Hydrol Res Lett 10:67–73

Zhang Q, Rodríguez-Lado L, Johnson CA, Xue H, Shi J, Zheng Q, Sun G (2016) Predicting the risk of arsenic contaminated groundwater in Shanxi Province. N China Environ Pollut 165:118